Extending sensitivity for low-mass neutral heavy lepton searches

Loretta M. Johnson and Douglas W. McKay
Department of Physics and Astronomy, University of Kansas, Lawrence, Kansas 66045

Tim Bolton
Department of Physics, Kansas State University, Manhattan, Kansas 66502

(Received 17 March 1997)

We point out the importance of two-body final states of weak isosinglet neutral heavy leptons predicted in several models of new physics beyond the standard model. We concentrate on muon-type neutral heavy leptons L_μ^0 with a mass $M<2$ GeV that can be searched for with increased sensitivity at a new round of neutrino experiments at CERN and Fermilab. Providing explicit decay rate formulas for the $ee\nu$, $e\mu\nu$, $\mu\mu\nu$, $\pi\mu$, $\rho\mu$, and $a_1\mu$ final states, we use general scaling features to estimate the sensitivity of L_μ^0 searches in current and future experiments, emphasizing the importance of the $\pi\mu$ decay mode. [S0556-2821(97)05717-2]

PACS number(s): 13.35.Hb, 14.60.St

I. INTRODUCTION

The $N_\nu = 3$ bound at the CERN e^+e^- collider LEP on the number of light, sequential-family neutrinos [1] tends to obscure the fact that relatively low-mass neutral leptons L^0 weakly mixed with one or more of e, μ, or τ neutrinos, are still allowed. Grand unified theory models provide motivation, since some models may contain rather light neutral leptons [2]. Here we are specifically interested in L^0 with a mass M of order 1 GeV, and we assume for simplicity that a given massive neutrino mixes with only one light neutrino flavor. Experimental bounds exist [3], but it is timely to revisit them in light of the high intensity neutrino experiments coming on line or under development and construction.

We especially emphasize the role of the $L^0\to\pi^\pm\ell^\mp$ ($\ell^\mp=e^\mp,\mu^\mp$) decay mode in greatly increasing the sensitivity of searches for L^0 with $M<1$ GeV, where phase space strongly favors this two-body mode. For $M>1$ GeV, the purely leptonic modes come into their own to provide clean signals for L^0 decays.

II. HEAVY NEUTRAL LEPTON AND DECAYS

A. Mixing

In this study we are concerned with the search for heavy neutral leptons which are primarily isosinglets under weak $SU(2)_L$. These can mix with the light neutrinos, which are doublet members under $SU(2)_L$. Whether the neutrinos are massless or massive but light, the mixing effect can be represented to a good approximation by replacing ν_{i_L}, $i=e,\mu,\tau$, by

$$(\mathcal{N}_i)_L \simeq (\nu_i)_L\left(1-\frac{\Sigma_a|\mathcal{U}_{ia}|^2}{2}\right)+\sum_a \mathcal{U}_{ia}(L_a^0)_L. \qquad (1)$$

Here, $(\nu_i)_L$ and $(L_a^0)_L$ are the left-handed components of the neutrinos and heavy neutral leptons, while $(\mathcal{N}_i)_L$ are the combinations that appear in the charged and neutral weak currents (the weak interaction ''eigenfields''). For simplicity, we consider the case where each ν_i mixes with only one L_i^0. If the neutrinos ν_i are massive, the mixing can be illustrated by a ''seesawlike'' mass matrix [4],

$$\mathcal{M}=\begin{pmatrix}0 & \lambda\\ \lambda & M\end{pmatrix}, \qquad (2)$$

where $\mathcal{M}$ has eigenvalues

$$m_\pm=\frac{M}{2}\left(1\pm\sqrt{1+\frac{4\lambda^2}{M^2}}\right), \qquad (3)$$

and corresponding eigenvectors

$$v_\pm=\left(\frac{\lambda}{\sqrt{m_\pm^2+\lambda^2}},\frac{m_\pm}{\sqrt{m_\pm^2+\lambda^2}}\right). \qquad (4)$$

When $\lambda/M\ll 1$, $L^0\equiv v_+\approx(\lambda/M,1-\lambda^2/2M^2)$ is associated with $m_+\approx M$, while $\nu\equiv v_-\approx(1-\lambda^2/2M^2,-\lambda/M)$ belongs to $m_\nu\equiv|m_-|\approx\lambda^2/M$. If, as in some specific models, λ were related to charged lepton or quark masses, the mixing parameter $U\simeq\lambda/M$ could be determined by the heavy neutral lepton mass alone.

In the work we present here, U and M are treated as independent parameters. Since our treatment is perturbative, the mixing indicated in Fig. 1 can be characterized by a mixing mass parameter λ, while the L^0 and ν lines represent propagators or a propagator and an external wave function. For example, treating L^0 decay, one has factors

$$\lambda\frac{\not p+m_\nu}{p^2-m_\nu^2}U_{L^0}(p)=\frac{\lambda}{M-m_\nu}U_{L^0}(p)\simeq\frac{\lambda}{M}U_{L^0}(p), \qquad (5)$$

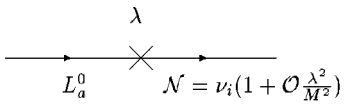

FIG. 1. L^0 mixing.

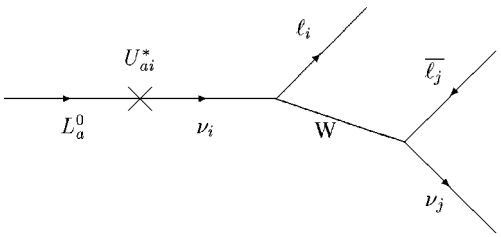

FIG. 2. L^0 charged current decay.

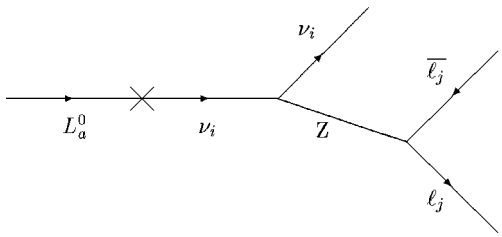

FIG. 3. L^0 neutral current decay.

where $U_{L^0}(p)$ is the L^0 momentum space wave function and $m_\nu/M \ll 1$. The parameters λ and M are to be determined, or bounded, by experiment.

Figures 2 and 3 show the Feynman diagrams for the charged and neutral current contributions to leptonic L^0_a decay in lowest order in U_{ia}'s and weak couplings.[1] For a final state where $\ell_i \neq \ell_j$ and both leptons are observed (which is required in the analysis presented here), only the charged current processes, Fig. 2, contribute. Assuming the charges of the final leptons are determined, say ℓ_i^- and ℓ_j^+, then there is a single diagram with factor U_{ia}. If the flavors, but not the charges, of the leptons are determined, one has a second mode and another diagram with ℓ_j^- at the upper vertex and ℓ_i^+ at the lower one. The decay involves two terms, one with a factor $|U_{ia}|^2$ and one with $|U_{ja}|^2$. For the $e\mu$ case, $\Gamma^{e^-\mu^+} = \Gamma^{\mu^- e^+}$, so $\Gamma^{e\mu} = (|U_e|^2 + |U_\mu|^2)\Gamma^{\mu^- e^+}$.

In the case that $\ell_i = \ell_j$, the neutral current diagrams are involved, and each ν_i can contribute for a fixed j and fixed a. There is only *one* charged current contribution, proportional to U_{aj}, in this instance. The diagram where $i=j$ in Fig. 3, also proportional to U_{aj}, interferes with that of Fig. 2, while the other two terms with $i \neq j$ contribute incoherently to the partial rate for $L^0_a \to \ell_j \overline{\ell_j} +$ missing neutrinos. We give the expressions for the muon-type L^0 in Appendix A. The numerical results and parameter bounds that we present will be for the situation where only muon neutrinos mix with a given heavy neutral lepton. The results can be generalized straightforwardly to the mixed cases.

While on the topic of mixing, it is worth offering the reminder that heavy neutral leptons with masses below 2 GeV will live long enough [5] to escape the LEP and SLAC Linear Collider (SLC) detectors before decaying and thus they are disguised within the $N_\nu = 3$ light-neutrino number measurements [1]. The right-handed components of L^0 do not couple to Z^0, while the left-handed components couple through the mixing displayed in Eq. (1) and in Fig. 1, which ensures that the ''missing'' decay partial width, which is proportional to $\Sigma_{i=1}^3 |(\overline{\mathcal{N}_i})_L (\mathcal{N}_i)_L|^2$, gives the usual result as long as L^0's are light enough to be treated to the accuracy of present measurements as massless particles in the final state.

[1]For definiteness we diagram the decay as if the source beam were Dirac neutral heavy leptons (NHL's). If the beam is sign selected (such as that of the NuTeV experiment [6], for example), then this case applies directly. If the neutral lepton source is from a beam dump (as in the DONUT experiment, for example), then there is a democratic mixture of neutrino and antineutrino; and the conjugate L^0's and consequent conjugate lepton final states are all present. For Majorana-type NHL, each charge state can occur in any decay regardless of the nature of the beam preparation, and the diagram with the lepton switched in Fig. 1 also occurs.

B. Decays

In this subsection, we present the partial decay widths of L^0 to channels of relevance for our study. For definiteness we restrict our attention to a ''μ-type'' L^0_μ that mixes only with the weak muon neutrino with mixing strength denoted by U.

1. Leptonic decays

Referring to Fig. 2, we see that the relevant decays are

$$L^0_\mu \to \mu^- e^+ \nu_e \tag{6}$$

and

$$L^0_\mu \to \mu^+ \mu^- \nu_\mu . \tag{7}$$

For convenience, we divide out a common factor

$$K \equiv \frac{G_F^2 M^5}{192\pi^3} U^2, \tag{8}$$

which happens to be equal to the all-neutrino decay rate summed over flavor,

$$K = \sum_{i=e,\mu,\tau} \Gamma(L^0_\mu \to \nu_\mu \nu_i \overline{\nu_i}), \tag{9}$$

where the Z^0 coupling factors and the identical particle effects for $i=\mu$ yield $K/2$, $K/4$, and $K/4$, for μ, e, τ, respectively. K is also equal to the usual μ-decay width formula when the electron mass is neglected, up to the factor U^2. Differential and integrated partial width formulas are summarized in Appendix A. Integrated partial widths, $\Gamma(L^0_\mu \to \mu^+ e^- \nu_e)/K$ and $\Gamma(L^0_\mu \to \mu^+ \mu^- \nu_\mu)/K$ are shown as a function of M, the L^0_μ mass, in Fig. 4. Clearly the three-body leptonic modes come into their own above $M = 1$ GeV, but the hadronic modes summarized next also play a major role in detection of L^0_μ decay.

2. Exclusive hadronic decays

The exclusive decays

$$L^0_\mu \to \mu^- H^+, \tag{10}$$

where $H = \pi$, ρ, or a_1, are large modes that can be reliably calculated within our framework. As we will explain in Sec. III B, only partial widths are needed for experimental

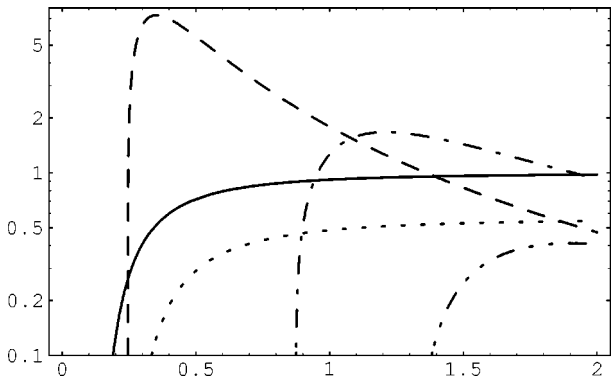

FIG. 4. The important leptonic and hadronic decay widths Γ/K as a function of M in GeV. The solid curve is the $e\mu\nu$ mode, dotted is $\mu\mu\nu$, dashed is $\pi\mu$, dot dashed is $\rho\mu$, and dot-dot dashed is $a_1\mu$. Note that the $\pi\mu$ peak is more than seven times higher than the $e\mu\nu$ peak.

searches since U is already constrained to be small. The signatures are clean, and the L_μ^0 detection sensitivity increases dramatically when these search modes are included, as we discuss in the following section. The isospin-related neutral modes $L_\mu^0 \to \nu_\mu H^0$ are not as useful experimentally, and are not explicitly included in the discussion.

The $L_\mu^0 \to \mu^- \pi^+$ partial width is fixed by $\pi^+ \to \mu^+ \nu_\mu$ while $\Gamma(L_\mu^0 \to \mu^- \rho^+)$ and $\Gamma(L_\mu^0 \to \mu^- a_1^+)$ are fixed by $\tau^+ \to \rho^+ \nu_\tau$ and $\tau^+ \to a_1^+ \nu_\tau$ decay. The ratios $\Gamma(L_\mu^0 \to \mu^- H^+)/K$ are shown in Fig. 4 as a function of M. The special prominence of the $L_\mu^0 \to \mu^- \pi^+$ mode for low mass L_μ^0 is evident. Regarding the interpretation of the figure, note that two-body decays *appear* to rise, peak, and fall as a function of M because of our normalization to the three-neutrino decay width K. Two-body decays are proportional to $G_F^2 M^3 f_H^2$, where $f_H = f_\pi$ in the pion case, for example. The peak in the curves for the π^+, ρ^+, and a_1^+ final state partial rates is then an artifact of the M^{-2} from our normalization multiplied by the rapidly rising two-body phase space.

As an aside, we note that two-body decays allow the potential discrimination between electron-type and muon-type NHL through the observation of $L_\mu^0 \to \mu^- H^+$ vs $L_e^0 \to e^- H^+$.

Next, we turn to a consideration of the issue of sensitivity to L_μ^0 detection in experimental searches, focusing on those aspects that follow from basic scaling considerations and are independent of details of specific experiments, which must be handled by thorough Monte Carlo analysis.

III. ESTIMATES OF SENSITIVITY

A. Production of L_μ^0 from meson decay

Light neutral heavy leptons could be produced in weak decays of charged mesons; $K^\pm$, $D^\pm$, and $D_S^\pm$ provide the most experimental sensitivity because they can be produced in an enormous quantity in the pN collisions that generate neutrino beams and because Cabibbo-Kobayashi-Maskawa suppression of the two-body decay is modest ($K^\pm$, $D^\pm$) or absent ($D_S^\pm$). The two-body decay rate [5] can be related directly to the $\mu\nu$ decay rate

$$\Gamma(H \to \mu L_\mu^0) = U^2 \Gamma(H \to \mu\nu) \times (M/M_\mu)^2 \eta_P(M/M_H, M_\mu/M), \tag{11}$$

where $H = (K^\pm, D^\pm, D_S^\pm)$, U^2 is the mixing factor, M_H is the meson mass, M is the L_μ^0 mass, M_μ is the muon mass, and

$$\eta_P(x,y) = \frac{[(1+y^2) - x^2(1-y^2)^2]\sqrt{[1-x^2(1-y)^2][1-x^2(1+y)^2]}}{(1-x^2y^2)^2} \tag{12}$$

is a kinematic factor. Note that for $M^2/M_\mu^2 \gg 1$, $y^{-2}\eta_P(M/M_H, M_\mu/M) \to (M/M_\mu)^2[1-(M/M_H)^2]^2$, demonstrating that two-body decays to L_μ^0 can be considerably enhanced by the lifting of helicity suppression.

B. Experimental detection of L_μ^0

The simplest scheme for a detector is a low-mass decay space immediately in front of a neutrino detector [6,7], instrumented with tracking chambers to permit reconstruction of a possible L_μ^0 decay vertex. By removing as much mass as possible, for example, through the use of helium-filled bags, backgrounds from conventional $\nu_\mu N$ interactions can be minimized. The neutrino detector downstream of the low-mass region can be used to identify muons, pions, and electrons and measure their energies, thus providing sensitivity to the largest decay modes of L_μ^0 with $M < 2$ GeV, $L_\mu^0 \to e\mu, \mu\mu, \pi\mu$. While a dedicated instrumented low-mass detector is optimal, it is not necessary, provided the density of material in front of the neutrino detector is not too high.

If a decay space is constructed to have a length Δ along the direction of the beam and a width much wider than the beam, the probability of a L_μ^0 being observed in the detector can be expressed as

$$P_D^{L_\mu^0}(M, U^2) = \int_{Z-\Delta/2}^{Z+\Delta/2} \frac{dz}{\gamma\beta c\,\tau_{L_\mu^0}} e^{-z/\gamma\beta c\,\tau_{L_\mu^0}} \frac{\Gamma_{L_\mu^0}^{\rm det}}{\Gamma_{L_\mu^0}^{\rm tot}} \varepsilon_D^{L_\mu^0}, \tag{13}$$

where $\Gamma_{L_\mu^0}^{\rm det}, \Gamma_{L_\mu^0}^{\rm tot}$ are the detected and total decay widths, z is the distance of the decay position from the L_μ^0 production point, Z is the distance from the production point to the center of the decay channel, β is the L_μ^0 speed in units with $c = 1$, $\gamma = 1/\sqrt{1-\beta^2}$, $\gamma\beta c\,\tau_{L_\mu^0}$ is the L_μ^0 mean decay length,

and $\varepsilon_D^{L_\mu^0}$ is the average L_μ^0 detection efficiency. Mixing angles of interest are sufficiently small and detectors are configured such that $\Delta \ll Z \ll \gamma\beta c\tau_{L_\mu^0}$. In this case, Eq. (13) simplifies to

$$P_D^{L_\mu^0}(M,U^2) = \frac{\Delta}{\gamma\beta c\tau_{L_\mu^0}} \frac{\Gamma_{L_\mu^0}^{\rm det}}{\Gamma_{L_\mu^0}^{\rm tot}} \varepsilon_D^{L_\mu^0} \tag{14}$$

$$= \frac{\Delta}{\gamma\beta} \frac{\Gamma_{L_\mu^0}^{\rm det}}{\hbar c} \varepsilon_D^{L_\mu^0}. \tag{15}$$

Since $\tau_{L_\mu^0}\Gamma_{L_\mu^0}^{\rm tot} = \hbar$, the observation probability calculation requires only knowledge of the partial decay widths of the channels being searched for, $\Gamma_{L_\mu^0}^{\rm det}$. As these partial widths can be reliably calculated, there should be little theoretical uncertainty in estimates of search sensitivity.

C. Sensitivity in (U^2, M) plane

The number of produced L_μ^0 will be proportional to the total number of protons on target, $N_{\rm POT}$, and a factor U^2M^2 from Eq. (11), assuming $M_\mu^2 \ll M^2 \ll M_H^2$. Using the simple $e\mu$ decay mode as an example, the detected partial width will be proportional to U^2M^5. The number of decays in the decay region is proportional to this partial width, to the length of the decay space Δ, and to an extra factor of M/E from time dilation, with E the L_μ^0 energy. Combining all effects together, the number of observed L_μ^0 has the dependence as in Eq. (B9) below:

$$N_{L_\mu^0}^{\rm obs} \propto \frac{N_{\rm POT}\Delta}{E} U^4 M^8. \tag{16}$$

If an experiment performs a search and observes a statistically significant L_μ^0 signal, then the experiment can determine both M, from the two-body semihadronic decays, and U^2 from a more detailed development of Eq. (16) (see Appendix B). On the other hand, if no candidates are observed, then the experiment can exclude a region in the (U^2, M) plane that from Eq. (16) will be bounded by a curve of the form $U^2M^4 =$ const, or more specifically, Eq. (B11) below. The minimum mixing factor sensitivity for fixed M will be proportional to $\sqrt{E/(N_{\rm POT}\Delta)}$ for an experiment that suffers no background. Greater sensitivity follows from increasing $N_{\rm POT}$ and Δ or decreasing E, but the gain is slow because of the square-root factor.

Adding the hadronic decay channels presented here is another way to improve the search limits. For these two-body modes, the region an experiment can explore is bounded by a curve of the form $U^2M^3 =$ const, as can be seen by comparing Eqs. (A16) and (A17) below.

D. Estimates of sensitivity for current and future neutrino experiments

This subsection summarizes predictions for two rather different experiments: NuTeV [8], a high energy deep inelastic scattering experiment with its neutrino detector located far from the production target, and DONUT [9], a high energy beam dump experiment with its detector 35 m from the neutrino production target. We also comment on prospects in lower energy experiments. A more detailed prescription for our estimates is given in Appendix B.

1. The NuTeV experiment

NuTeV has installed an instrumented decay channel to search for neutral heavy leptons (NHL's) [6] and is currently taking data. The 40 m long NHL decay channel is located approximately 1200 m from the decay position for charmed mesons and 900–1200 m for charged kaons. NuTeV may receive an integrated intensity of up to 6×10^{18} protons on target. Neutrino interactions occur at a rate of approximately $20/10^{13}$ POT. The ratio of kaons to pions in the NuTeV beam is about 0.4 resulting in ν_e/ν_μ interaction ratio of about 2.3% in the detector. Contributions from charmed meson decay increase the ν_e rate by approximately 1% of itself. The Lab E neutrino detector used by NuTeV has a fiducial length of approximately 15 m and a mean density of 4.2 g/cm^3.

Figure 5 shows the estimate of sensitivity as a function of mass M (in GeV) to NHL's produced from kaon decay in NuTeV, as determined from Eq. (B11) below. The vertical axis represents the minimum mixing parameter $|U|^2$ the experiment would be sensitive to from kaon decays alone assuming no candidate events were observed (and no background events were expected) in an exposure to 6×10^{18} protons on target. The dashed, solid, and dot-dashed curves are for kaon energies of 100, 150, and 200 GeV, respectively, and assume the search is performed only using the $L_\mu^0 \to e\mu$ decay mode. The dotted curve illustrates the sensitivity that could be gained for 150 GeV kaon energy if the $\pi\mu$, $\rho\mu$, and $a_1\mu$ modes were added to the $e\mu$ mode in the search. The main model sensitivity comes from the assumption for the mean K^+ energy, which enters both in the lifetime calculation of the L_μ^0 and the interaction probability for the neutrinos used in the normalization sample.

Figure 6 shows a plot similar to that in Fig. 5 for NHL's produced from $D_S^\pm$ decay [Eq. (B23) below]. The vertical axis represents the minimum mixing parameter $|U|^2$ the experiment would be sensitive to from D_S decays alone assuming no candidate events were observed (and no background events were expected) in an exposure to 6×10^{18} protons on target. The dashed, solid, and dot-dashed curves are for charmed hadron energies of 50, 100, and 200 GeV, respectively, and assume the search is performed only using the $L_\mu^0 \to e\mu$ decay mode. The dotted curve illustrates the sensitivity that could be gained for 100 GeV D_S energy if the $\pi\mu$, $\rho\mu$, and $a_1\mu$ modes were added to the $e\mu$ mode in the search. The main model sensitivity in this result comes from the assumption for the mean D_S^+ energy.

Figure 7 shows the estimated sensitivity for all modes combined using either the $e\mu$ decay channel by itself or the $e\mu$, $\pi\mu$, $\rho\mu$, and $a_1\mu$ channels combined. The vertical axis represents the minimum mixing parameter $|U|^2$ the experiment would be sensitive to from all meson decays combined assuming no candidate events were observed (and no background events were expected). The curves assume 6×10^{18} POT, a mean kaon energy of 150 GeV, and a mean charmed

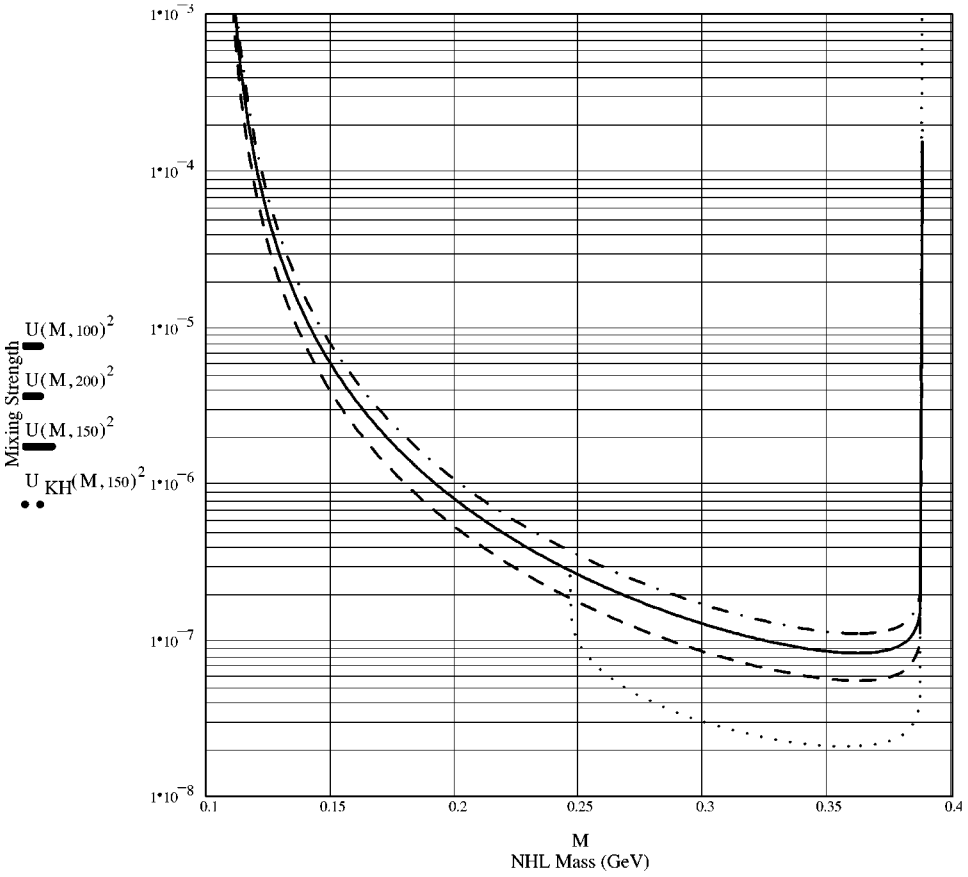

FIG. 5. Estimated sensitivity plot in U_K^2 vs M for NHL's produced from $K^{\pm}$ decay in NuTeV. The dashed, solid, and dot-dashed curves are for kaon energies of 100, 150, and 200 GeV, respectively, and assume the search is performed only using the $L_\mu^0 \to e\mu$ decay mode.

meson energy of 100 GeV. The solid curve shows the expected result assuming the search was performed only using the $L_\mu^0 \to e\mu$ decay mode. The dotted curve illustrates the sensitivity that could be gained by adding the $\pi\mu$, $\rho\mu$, and $a_1\mu$ modes to the search. Note that the U^4 dependence of the detection rate for NHL's implies that uncertainties in acceptances, branching fractions, etc., which only enter as ratios, affect results only as square roots in determining U^2.

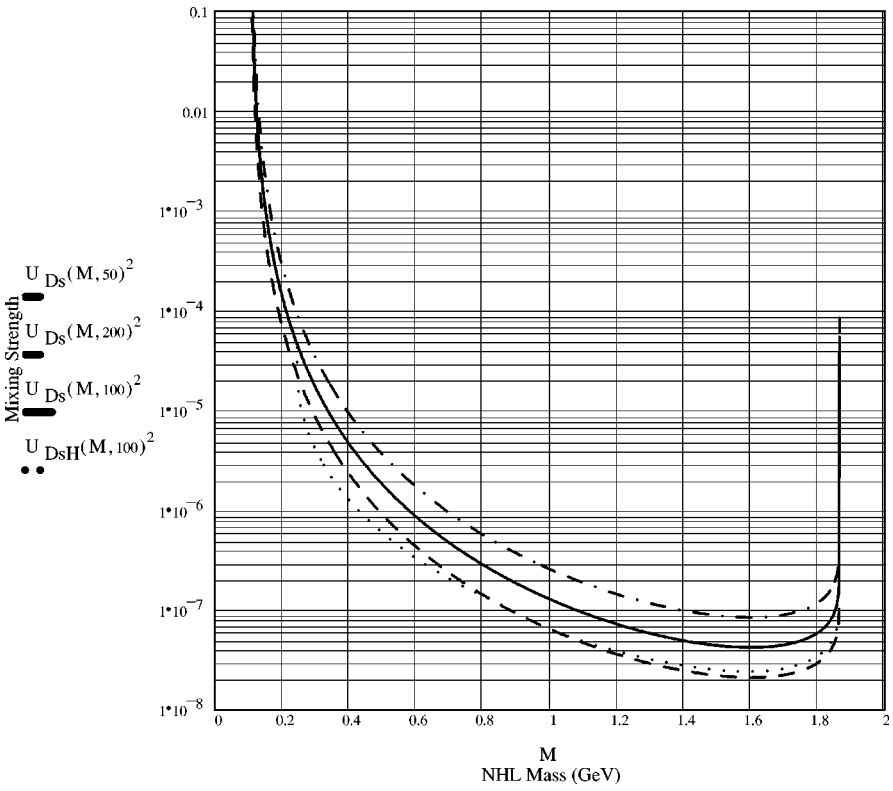

FIG. 6. Estimate of sensitivity as a function of mass M (in GeV) to NHL's produced from D_S decay in NuTeV. The dashed, solid, and dot-dashed curves are for charmed hadron energies of 50, 100, and 200 GeV, respectively, and assume the search is performed only using the $L_\mu^0 \to e\mu$ decay mode.

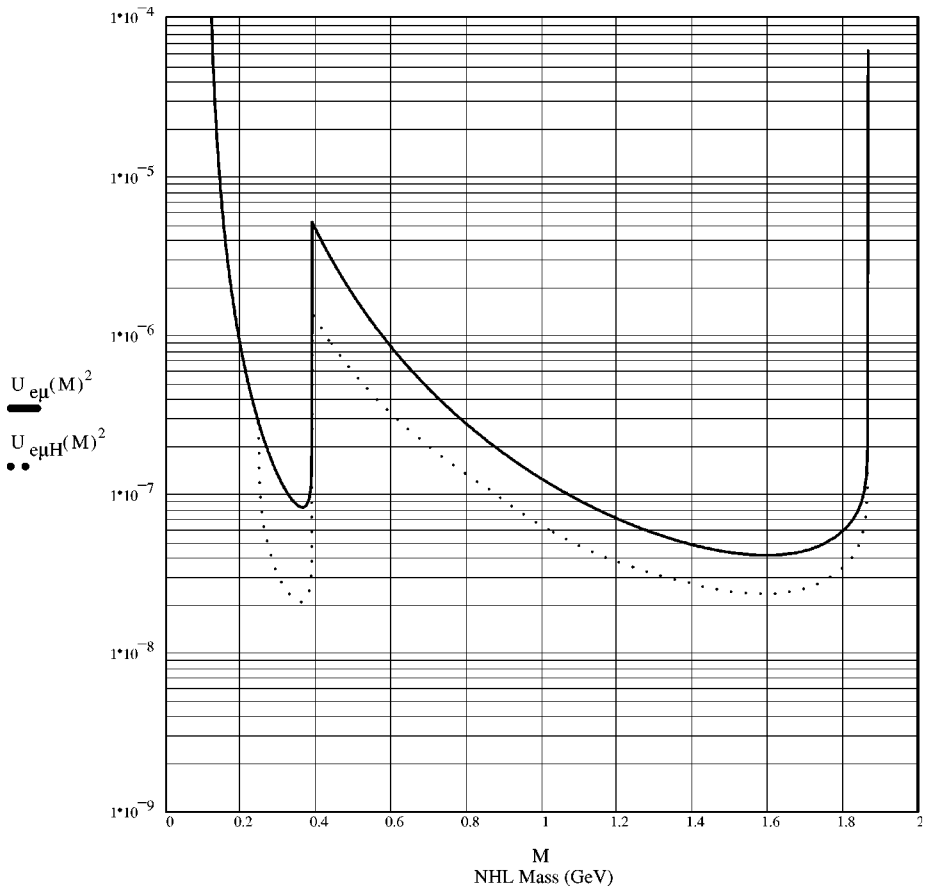

FIG. 7. Estimate of combined sensitivity to NHL's from K, D, and D_S decays in NuTeV as a function of NHL mass M (in GeV). The solid curve shows the expected result assuming the search was performed only using the $L^0_\mu \to e\mu$ decay mode. The dotted curve illustrates the sensitivity that could be gained by adding the $\pi\mu$, $\rho\mu$, and $a_1\mu$ modes to the search.

The dependence of the result on statistics, assuming no background, is similarly proportional to $1/\sqrt{N_{\rm POT}}$.

2. The DONUT experiment

DONUT is a hybrid emulsion spectrometer detector sited approximately 35 m from a beam-dump target in Fermilab's 800 GeV proton beam. Active and passive shielding eliminate essentially all neutrinos produced by pion and kaon decay, leaving a mixed beam of ν_e, ν_μ, and ν_τ from charmed hadron decay. The experiment's primary goal is to detect charged current interactions of ν_τ with nucleons in the emulsion target. DONUT may receive an exposure of up to 2×10^{18} protons on target.

DONUT's proximity to the production target greatly enhances the flux of neutrinos, and possible NHL's, produced from $D^\pm$ and $D_S^\pm$ decay. Only a few thousand charged current interactions in the emulsion detector are expected, but these will essentially all originate from charm decay. Figure 8 shows an estimate to sensitivity [10] for NHL's in DONUT, assuming the experiment could instrument a 5 m decay space in front of their emulsion target, and that the experiment receives an exposure of 2×10^{18} POT. The estimate is comparable to that for NuTeV, and possibly better at high L^0_μ mass.

3. Other experiments

We have used the NuTeV and DONUT experiments as specific examples in calculating sensitivity to NHL's; however, our formulas can easily be applied in other cases. CHORUS [11], also a hybrid emulsion spectrometer, and NOMAD [12], a low-mass high-resolution spectrometer, are running in a low energy horn beam at CERN to search for ν_τ produced from $\nu_\mu \to \nu_\tau$ oscillations. Two additional $\nu_\mu \to \nu_\tau$ oscillation experiments, COSMOS [13] and MINOS [14] at Fermilab, will begin taking data around 2001. All of these experiments can search for NHL's produced from (primarily) kaon decay because of their lower energy beams. We note that searches in this mass regime benefit appreciably from an ability to detect the $\pi\mu$ decay mode.

IV. SUMMARY

As just discussed, a number of Fermilab and CERN neutrino oscillation experiments are currently running or will soon come on line, and we have shown that a simple and direct method to expand the search for light ($M<2$ GeV) NHL's is suitable for all of these experiments. The present lower limits on lifetimes for NHL's in this mass range means that all experiments satisfy the criterion that $\Delta \ll z \ll \gamma\beta c\tau_{L^0}$ where Δ is the fiducial length, z is the source-to-detector distance, and $\gamma\beta c\tau$ is the decay length. Therefore, the simple criterion (14) applies. Only theoretical values of the partial widths into search modes are relevant, and these can be reliably calculated in terms of the mass and mixing parameters.

In addition to common features that lend themselves to a clean analysis, we have shown how important the two-body decay modes are, especially the $\pi\mu$ mode, in achieving improvements in sensitivity. We found significant gains over most of the mass range $M<2$ GeV, which means discovery

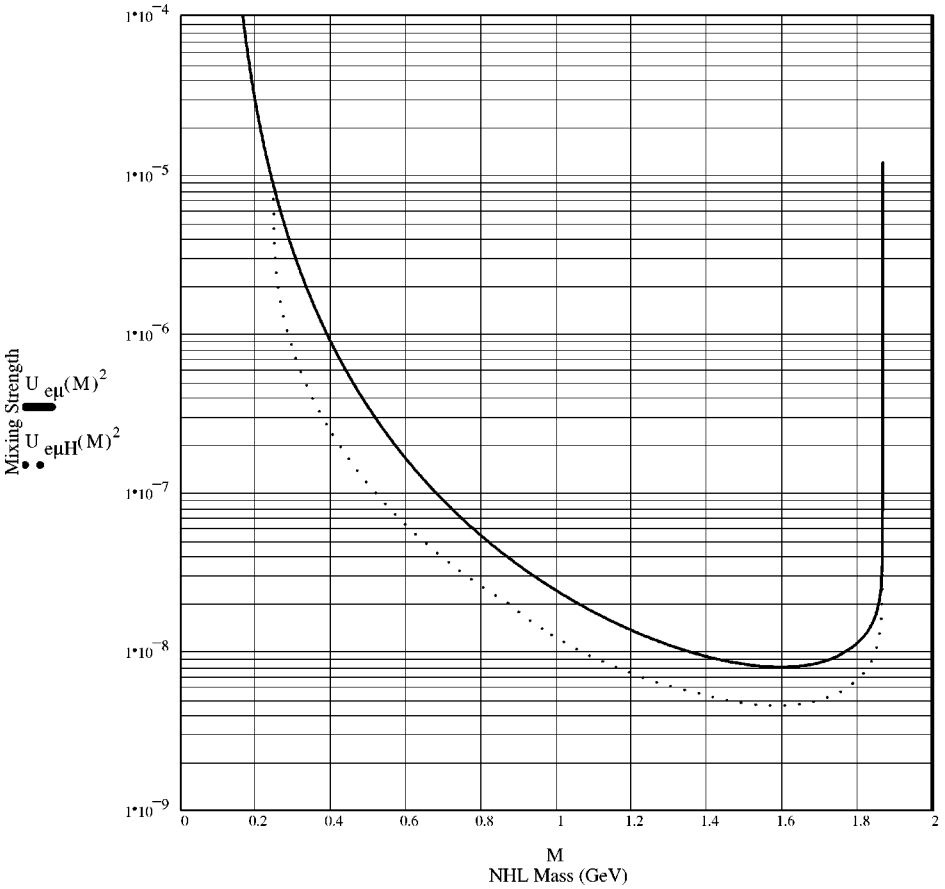

FIG. 8. Estimate of combined sensitivity to NHL's from D and D_S decays in DONUT as a function of NHL mass M (in GeV). The vertical axis represents the minimum mixing parameter $|U|^2$ the experiment would be sensitive to from all meson decays combined assuming no candidate events were observed (and no background events were expected). The curves assume 2×10^{18} POT and a mean charmed meson energy of 100 GeV. The solid curve shows the expected result assuming the search was performed only using the $L_\mu^0\to e\mu$ decay mode. The dotted curve illustrates the sensitivity that could be gained by adding the $\pi\mu$, $\rho\mu$, and $a_1\mu$ modes to the search.

reach extends to smaller mixing values than those currently reported in the literature.

Individual experiments will use sophisticated Monte Carlo simulations to properly account for details such as efficiencies and fluxes; but the simple and general formalism we have presented applies to all experiments. We believe our results provide a broad, useful framework for expanding searches for neutral heavy leptons.

ACKNOWLEDGMENTS

T.B. would like to thank Janet Conrad for numerous discussions about the NuTeV decay channel project. L.M.J. acknowledges support from the University of Kansas Graduate Summer program. D.W.M. thanks S. Randjbar-Daemi and Faheem Hussain for the hospitality of the high energy group at ICTP, Trieste. This work was supported in part by U.S. DOE Grants Nos. DE-FG02-85ER40214 and DE-FG02-94ER40814.

APPENDIX A: EXPLICIT DECAY RATE FORMULAS

In this appendix we collect formulas for partial decay widths to which we refer in the text. For completeness we also include the differential forms before the final integrations, including effects of L^0 polarization in the $e\mu$ decay channel. All formulas refer to the L^0 rest frame.

1. Leptonic rates

Referring to Fig. 2 and identifying $\mu^-=\ell_i$ and $e^+=\overline{\ell_j}$, with $x_\mu\equiv 2E_\mu/M$, $x_e\equiv 2E_e/M$, and $x_m\equiv M_\mu/M$, we have

$$\frac{d^2\Gamma^{(\mu^- e^+)}}{dx_e dx_\mu}=\frac{G_F^2M^5}{16\pi^3}|U_\mu|^2[x_e(1-x_e-x_m^2)], \qquad \text{(A1)}$$

where M is the L^0 mass, M_μ is the muon mass, and E_e and E_μ are the positron and muon energies. We have neglected the electron mass in writing Eq. (A1). Saving the x_μ integration until last, and setting $m_e=0$ in the phase-space treatment, the single differential decay form is given by the expression

$$\frac{d\Gamma^{(\mu^- e^+)}}{dx_\mu}=\frac{G_F^2M^5}{16\pi^3}|U_\mu|^2[-\tfrac{2}{3}x_m^2+\tfrac{1}{2}(1+x_m^2)x_\mu-\tfrac{1}{3}x_\mu^2]\times\sqrt{x_\mu^2-4x_m^2}. \qquad \text{(A2)}$$

Integrating over x_μ from $2x_m\leqslant x_\mu\leqslant 1+x_m^2$, we get the result familiar from muon decay,

$$\Gamma^{(\mu^- e^+)}=\frac{G_F^2M^5}{192\pi^3}|U_\mu|^2(1-8x_m^2+8x_m^6-x_m^8-12x_m^4\ln x_m^2). \qquad \text{(A3)}$$

For completeness we include the corresponding expressions for the $L_e^0\to e^-\mu^+\nu_\mu$ final state:

$$\frac{d^2\Gamma^{(e^-\mu^+)}}{dx_e dx_\mu}=\frac{G_F^2M^5}{16\pi^3}|U_e|^2[x_\mu(1-x_\mu+x_m^2)], \qquad \text{(A4)}$$

where again the electron mass is neglected. Integrating over the electron energy first, we obtain

$$\frac{d\Gamma^{(e^-\mu^+)}}{dx_\mu}=\frac{G_F^2M^5}{16\pi^3}|U_e|^2x_\mu(1-x_\mu+x_m^2)\sqrt{x_\mu^2-4x_m^2}. \tag{A5}$$

Comparing Eqs. (A2) and (A4), we see the interesting feature that, in principle, the difference in the two distributions could distinguish $L_\mu^0\to\mu^-e^+\nu_e$ from $L_e^0\to e^-\mu^+\nu_\mu$ even if the charge states were not determined directly. This is true even if $x_m<<1$, though distinguishing between distributions $\Gamma^{(\mu^-e^+)}\sim x_\mu^2-\frac{2}{3}x_\mu^3$ and $\Gamma^{(e^-\mu^+)}\sim x_\mu^2-x_\mu^3$ may be difficult. Integrating over the muon energy, one finds Eq. (A3).

If the L_μ^0 is produced through meson decay, it will likely be highly polarized. Correlations between the polarization vector and the e and μ momentum vectors could produce substantial effects in detection efficiency for the $L_\mu^0\to\mu^-e^+\nu_e$ final state. To permit study of these effects, we give the following triply differential decay formulas:

$$\frac{d^3\Gamma^{(\mu^-e^+)}}{dx_\mu dx_e d\cos\theta_e}=\frac{G_F^2M^5}{32\pi^3}|U_\mu|^2x_e(1-x_m^2-x_e)(1+\cos\theta_e), \tag{A6}$$

where θ_e is the angle between the final e^+ direction and the polarization direction of the decaying L^0, and m_e is neglected as before; or, alternatively,

$$\frac{d^3\Gamma^{(\mu^-e^+)}}{dx_\mu dx_e d\cos\theta_\mu}=\frac{G_F^2M^5}{32\pi^3}|U_\mu|^2x_e(1-x_m^2-x_e)\times(1+\cos\widetilde{\theta}_e\cos\theta_\mu), \tag{A7}$$

where

$$\cos\widetilde{\theta}_e=\frac{(2-x_\mu-x_e)^2-x_\mu^2-x_e^2+4x_m^2}{2x_e\sqrt{x_\mu^2-4x_m^2}} \tag{A8}$$

and θ_μ is the angle between the final μ^- direction and the polarization direction of the decaying L^0.

Turning to the case where there are two muons in the final state and the charged and neutral current contributions interfere, we write the double differential decay formula as

$$\frac{d^2\Gamma^{(\mu^-\mu^+)}}{dx_+dx_-}=\frac{G_F^2M^5}{64\pi^3}|U_\mu|^2[x_+(1-x_+)(a+b)^2+x_-(1-x_-)(a-b)^2+2x_m^2(2-x_--x_+)(a^2-b^2)], \tag{A9}$$

where $x_\pm=2E_{\mu^\pm}/M$, $a=(3/2-2\sin^2\theta_W)$, $b=1/2$, and $\sin^2\theta_W\cong0.224$. Integrating over x_+, one obtains

$$\frac{d\Gamma^{(\mu^-\mu^+)}}{dx_-}=\frac{G_F^2M^5}{16\pi^3}|U_\mu|^2\{[x_-(1-x_-)(a-b)^2+2x_m^2(2-x_-)(a^2-b^2)](x_-^u-x_-^\ell)+\tfrac{1}{2}[(a+b)^2-2x_m^2(a^2-b^2)][(x_-^u)^2-(x_-^\ell)^2]-\tfrac{1}{3}(a+b)^2[(x_-^u)^3-(x_-^\ell)^3]\}. \tag{A10}$$

The expressions for x_-^u and x_-^ℓ in Eq. (A10) read

$$x_-^{u,\ell}=\frac{\left[-\left(\frac{x_-}{2}-1\right)(1-x_-+2x_m^2)\pm\frac{1}{2}\sqrt{x_-^2-4x_m^2}(1-x_-)\right]}{(1+x_m^2-x_-)}. \tag{A11}$$

One obtains the corresponding expression for $d\Gamma^{(\mu^-\mu^+)}/dx_+$ by the replacement $x_-\to x_+$. Integrating the expression (A10) over x_-, one obtains the partial width formula for $L_\mu^0\to\mu^-\mu^+\nu_\mu$: namely,

$$\Gamma^{(\mu^-\mu^+)}=\frac{G_F^2M^5}{192\pi^3}|U_\mu|^2\{C_1[(1-14x_m^2-2x_m^4-12x_m^6)\sqrt{1-4x_m^2}+12x_m^4(x_m^4-1)L]+4C_2[x_m^2(2+10x_m^2-12x_m^4)\sqrt{1-4x_m^2}+6x_m^4(1-2x_m^2+2x_m^4)L]\}, \tag{A12}$$

where

$$L=\ln\left[\frac{1-3x_m^2-(1-x_m^2)\sqrt{1-4x_m^2}}{x_m^2(1+\sqrt{1-4x_m^2})}\right]. \tag{A13}$$

The coefficients C_1 and C_2 in Eq. (A12) are

$$C_1=\tfrac{1}{4}[1+4\sin^2\theta_W+8\sin^4\theta_W], \tag{A14}$$

$$C_2=\tfrac{1}{2}\sin^2\theta_W[1+2\sin^2\theta_W]. \tag{A15}$$

For completeness we give the corresponding $L_\mu^0\to e^+e^-\nu_\mu$ partial width

$$\Gamma^{(e^-e^+)}=\frac{G_F^2M^5}{192\pi^3}|U_\mu|^2\tfrac{1}{4}[1-4\sin^2\theta_W+8\sin^4\theta_W]. \tag{A16}$$

2. Two-body hadronic decay formulas

The three decay modes of interest in this work are $L_\mu^0 \to \pi^+ \mu^-$, $\rho^+ \mu^-$, and $a_1^+ \mu^-$, which involve the decay constants f_π, g_ρ, and g_a. We determine g_ρ and g_a from the partial widths for $\tau \to \rho \nu_\tau$ and $\tau \to a_1 \nu_\tau$ using the lowest order diagrams. As justification, we note that the $\tau \to \pi \nu_\tau$ partial width calculated using the measured value of f_π agrees with the experiment to within a few percent. The decay formulas in the rest frame of L^0 read, in the narrow ρ, a_1 width approximation,

$$\frac{d\Gamma^{(\pi\mu)}}{d\Omega} = f_\pi^2 \frac{\cos^2\theta_c}{64\pi^2} G_F^2 |U_\mu|^2 M^3 \sqrt{\mathcal{S}(M, M_\pi, M_\mu)} \times \left[\left(1 - \frac{M_\mu^2}{M^2} \right)^2 - \frac{M_\pi^2}{M^2} \left(1 + \frac{M_\mu^2}{M^2} \right) \right], \tag{A17}$$

$$\frac{d\Gamma^{(\rho\mu)}}{d\Omega} = \frac{g_\rho^2}{M_\rho^2} \frac{\cos^2\theta_c}{32\pi^2} G_F^2 |U_\mu|^2 M^3 \sqrt{\mathcal{S}(M, M_\rho, M_\mu)} \times \left[\left(1 + \frac{M_\mu^2}{M^2} \right) \frac{M_\rho^2}{M^2} - 2\frac{M_\rho^4}{M^4} + \left(1 - \frac{M_\mu^2}{M^2} \right)^2 \right], \tag{A18}$$

where

$$\mathcal{S}(M, M_H, M_\mu) = \left[1 - \left(\frac{M_H}{M} - \frac{M_\mu}{M} \right)^2 \right] \left[1 - \left(\frac{M_H}{M} + \frac{M_\mu}{M} \right)^2 \right] \tag{A19}$$

and $d\Gamma^{(a_1\not)}/d\Omega$ is obtained from Eq. (A18) with the replacements $g_\rho \to g_a$ and $M_\rho \to M_a$. The integrated partial widths are obviously obtained by multiplying Eqs. (A17) and (A18) by 4π.

The parameters g_ρ and g_a are determined from the τ partial widths [15] to be

$$g_\rho^2 = \frac{\Gamma(\tau \to \rho \nu_\tau)}{\frac{G_F^2}{8\pi} \cos^2\theta_c \frac{M_\tau^3}{M_\rho^2} \left(1 - \frac{M_\rho^2}{M_\tau^2} \right) \left(1 + \frac{2M_\rho^2}{M_\tau^2} \right)} = (0.102\ \text{GeV}^2)^2, \tag{A20}$$

and similarly

$$g_a^2 = (0.128\ \text{GeV}^2)^2. \tag{A21}$$

The branching fraction for $\tau^- \to \pi^- \pi^+ \pi^- + \geq 0$ neutrals $+ \nu_\tau$ was used for the a_1 fraction. A recent chiral dynamics analysis of mesons [16] yields

$$g_\rho = 0.104\ \text{GeV}^2 \tag{A22}$$

and

$$g_a = 0.136\ \text{GeV}^2, \tag{A23}$$

in reasonable agreement with the values in Eqs. (A20) and (A21).

APPENDIX B: DETAILED ESTIMATES OF SENSITIVITY

A useful way to estimate sensitivity to NHL couplings is to normalize to neutrino interactions in the detector produced by the same parent meson as that which produces the NHL's. This technique relies less on absolute calculations from a beam Monte Carlo simulation and allows one to identify important model dependencies.

This appendix will develop estimates of sensitivity to NHL's produced from $K^\pm$, $D^\pm$, and $D_S^\pm$ two-body meson decays.

1. μ-type NHL's from kaons

We define the observable

$$R_K(M, U^2) = \frac{\text{Detected } L_\mu^0 \text{ in channel from } K^+ \text{ decays}}{\text{Detected } \nu_\mu \text{ in detector from } K^+ \text{ decays}} = R_P(M, U^2) R_B(M, U^2) R_D(M, U^2), \tag{B1}$$

with $R_P(M, U^2)$, $R_B(M, U^2)$, and $R_D(M, U^2)$ defined as the L_μ^0 production ratio, beam transport ratio, and detection ratio, respectively. The number of detected L_μ^0 will be a strong function of L_μ^0 mass M and mixing factor U^2. The number of ordinary ν_μ detected from K^+ decays can be inferred from the energy spectrum of neutrino interactions in the neutrino detector. By formulating the search as a measurement of the ratio $R_K(M, U^2)$, one lessens sensitivity to absolute normalization of the neutrino beam and detector acceptance. To establish the limits of experimental sensitivity, we will consider the null case, where no L_μ^0 candidates are observed for a given exposure in a neutrino beam. In this case, the upper 90% confidence level limit sensitivity for $R_K(M, U^2)$ follows, assuming no observed events and no background, from Poisson statistics,

$$R_K(M, U^2) \leq \frac{2.3}{r_{K\pi} n_{\nu_\mu} N_{\text{POT}}}, \tag{B2}$$

with $r_{K\pi}$ the fraction of ν_μ events from kaons, n_{ν_μ} the number of ν_μ interactions in the detector per incident proton, and N_{POT} the total number of protons on the production target. This section will derive the functional dependence of $R_K(M, U^2)$ on M and U^2 that will allow limits to be placed on the (M, U^2) plane from a null result search.

a. Production factor $R_P(M, U^2)$

$R_P(M, U^2)$ is the ratio of produced NHL's to produce ν_μ from kaons [5]:

$$R_P(M, U^2) = \frac{U^2 M^2}{M_\mu^2} \eta_P \left(\frac{M}{M_K}, \frac{M_\mu}{M} \right), \tag{B3}$$

where, as before, U is the ν_μ-L_μ^0 mixing strength, η_P is defined in Eq. (12), and M, M_μ, and M_K are the NHL, muon, and charged kaon masses, respectively.

b. Beam factor $R_B(M,U^2)$

$R_B(M,U^2)$ is the relative acceptance for NHL's vs neutrinos due to the beamline. An experiment will generally run a detailed Monte Carlo simulation to obtain this factor, but at high energies, $E_{L^0_\mu} \gg M$, one would expect only modest acceptance differences. Accordingly, we assume for estimation purposes that

$$R_B(M,U^2) = \frac{\varepsilon_B^{L^0_\mu}}{\varepsilon_B^{\nu_K}} \approx 1.0. \tag{B4}$$

c. Detection factor $R_D(M,U^2)$

$R_D(M,U^2)$ is the relative detection probability for NHL's vs ν_μ. This can be expressed as a ratio of detection probabilities,

$$R_D(M,U^2) = \frac{P_D^{L^0_\mu}(M,U^2)}{P_D^{\nu_K}}. \tag{B5}$$

For a long NHL lifetime, the NHL detection probability $P_D^{L^0_\mu}(M,U^2)$ can be written as in Eq. 14:

$$P_D^{L^0_\mu}(M,U^2) = \frac{\Delta}{\gamma\beta c\,\tau_{L^0_\mu}} \frac{\Gamma_{L^0_\mu}^{\rm det}}{\Gamma_{L^0_\mu}^{\rm tot}} \varepsilon_D^{L^0_\mu}, \tag{B6}$$

where $\Gamma_{L^0_\mu}^{\rm det}, \Gamma_{L^0_\mu}^{\rm tot}$ are the detected and total decay widths, Δ is the length of the decay channel, $\gamma\beta c\,\tau_{L^0_\mu}$ is the L^0_μ decay length, and $\varepsilon_D^{L^0_\mu}$ is the mean L^0_μ detection efficiency, assumed to be 1.0. Choosing to observe only the $e\mu$ mode for simplicity, $P_D^{L^0_\mu}(M,U^2)$ can be reexpressed as

$$P_D^{L^0_\mu}(M,U^2) = \frac{U^2 M^6 \Delta}{\langle E_{L^0_\mu}\rangle M_\mu^5 c\,\tau_\mu \hbar} \varepsilon_D^{L^0_\mu} \eta_D(M_\mu/M), \tag{B7}$$

with $\eta_D(M_\mu/M)$ a threshold factor in the L^0_μ decay that can be read from Eq. (A3) for the $e\mu$ decay.

The neutrino interaction probability is simply

$$P_D^{\nu_K}(M,U^2) = N_A \langle \rho t\rangle \sigma'_\nu \langle E_\nu\rangle \varepsilon_D^{\nu_K}, \tag{B8}$$

where $\sigma'_\nu\langle E_\nu\rangle = 0.68\times 10^{-38}\langle E_\nu\rangle$ cm^2 is the neutrino-nucleon cross section, $N_A\langle\rho t\rangle$ is the target thickness in units of nucleons/cm, and $\varepsilon_D^{\nu_K}$ is the target detection efficiency, which is usually close to 1.0.

d. Sensitivity formula

The final prediction for $R_K(M,U^2)$ is of the form

$$R_K(M,U^2) = CU^4M^8, \tag{B9}$$

with C containing all experiment-specific information,

$$C = a\frac{\eta_P\left(\frac{M}{M_K},\frac{M_\mu}{M}\right)\eta_D\left(\frac{M_\mu}{M}\right)\varepsilon_D^{L^0_\mu}\Delta}{\langle E_{L^0_\mu}\rangle\langle E_\nu\rangle\varepsilon_D^{\nu_K}\langle\rho t\rangle},$$

and a a constant,

$$a = [M_\mu^7 c\,\tau_\mu N_A \sigma'_\nu]^{-1} = 2.7\times 10^{16}\ \ {\rm cm}^{-3}\,{\rm g}^{-1}\,{\rm GeV}^{-6}. \tag{B10}$$

For fixed M, it follows from combining Eq. (B9) with Eq. (B2) that

$$U_K^2 \leqslant M^{-4}\sqrt{\frac{1}{C}\frac{2.3}{r_{K\pi} n_{\nu_\mu} N_{\rm POT}}}. \tag{B11}$$

This formula demonstrates the qualitative feature of any NHL's limit based on a search for decay vertices of NHL produced from meson decay. Sensitivity to the mixing U_K^2 is proportional to M^{-4} up to masses near the kinematic limit. The M^{-4} behavior originates from the U^4M^8 dependence of $R_K(M,U^2)$, with U^2M^2 arising from NHL production, U^2M^5 from NHL decay, and an extra factor of M from time dilation. Because of the U^4 dependence of $R_K(M,U^2)$, limits on U^2 only improve as the square root of the total integrated protons on target. The square root also ensures that other experimental effects, which enter as ratios in C, only weakly affect the sensitivity estimate.

Note that a formula similar to Eq. (B11) follows from analysis of the $\mu\pi$ final state, for example, but with M^{-3} appearing on the right-hand side and an η_D expression that can be read off from Eq. (A17).

2. μ-type NHL's from D^+ mesons

The calculation proceeds in a manner similar to the kaon case, except this time a more convenient normalization is relative to electron neutrinos from charmed mesons:

$$R_C(M,U^2) = \frac{\text{Detected } L^0_\mu \text{ in channel from } D^+ \text{ decays}}{\text{Detected } \nu_e \text{ in detector from } D^+ \text{ decays}} = R'_P(M,U^2)R'_B(M,U^2)R'_D(M,U^2). \tag{B12}$$

This choice is motivated by the fact that charm decays produce a negligible fraction of the total ν_μ, but on the order of 1% of the ν_e in a high energy beam. The 90% C.L. Poisson sensitivity to $R_C(M,U^2)$ can be written as

$$R_C(M,U^2) \leqslant \frac{2.3}{f_{\nu_e D} f_{\nu_e} n_{\nu_\mu} N_{\rm POT}}, \tag{B13}$$

where f_{ν_e} is the fraction of neutrino events which are ν_e and $f_{\nu_e D}$ is the fraction of interacting electron neutrinos from D^+ decay. Note that $f_{\nu_e D}\to 1$ in an ideal beam-dump experiment, whereas $f_{\nu_e D}\simeq 0.01$ in a conventional high energy experiment.

For the production rate, one can assume that all conventional ν_e are produced from three-body semileptonic decays whereas the NHL production is dominantly two body,

$$R'_P(M,U^2)=\frac{U^2M^2}{M_\mu^2}\,\eta_P\left(\frac{M}{M_D},\frac{M_\mu}{M}\right)\frac{B(D^+\to\mu^+\nu_\mu)}{B(D^+\to\mu^+X)}. \tag{B14}$$

In this formula the muon mass can be neglected compared to the D^+ mass M_D, and the ratio $B(D^+\to\mu^+\nu_\mu)/B(D^+\to\mu^+X)$ corrects for the use of three-body decays of the D^+ as the dominant source of ν_e. The D^+ muonic rate can be calculated assuming a D meson decay constant f_D [17] via $B(D^+\to\mu^+\nu_\mu)=(3.2\times10^{-4})(f_D/200\ \text{MeV})^2$, and the semimuonic rate $B(D^+\to\mu^+X)$ is measured as $B(D^+\to\mu^+X)=0.172$.

For the beam transport factor, we assume again a value of

$$R'_B(M,U^2)=1.0. \tag{B15}$$

This number may be less than 1.0 owing to the higher p_T given to the L_μ^0 relative to the three-body decay neutrino.

The detection factor is modified by the softer D^+ spectrum, relative to kaons, and the somewhat higher L_μ^0 energy expected relative to the ν_e from three-body decay. Again, take

$$R'_D(M,U^2)=\frac{P_D'^{L_\mu^0}(M,U^2)}{P_D'^{\nu_{eD}}}, \tag{B16}$$

with

$$P_D'^{L_\mu^0}(M,U^2)=\frac{U^2M^6\Delta}{\langle E'_{L_\mu^0}\rangle M_\mu^5 c\tau_\mu}\varepsilon_D^{L_\mu^0}\eta_D\left(\frac{M_\mu}{M}\right) \tag{B17}$$

and

$$P_D'^{\nu_{eD}}(M,U^2)=\langle\rho t\rangle\sigma'_\nu\langle E_{\nu_eD}\rangle N_A\varepsilon_D^{\nu_{eD}}. \tag{B18}$$

The final expression for $R_C(M,U^2)$ is

$$R_C(M,U^2)=C'U^4M^8, \tag{B19}$$

with

$$C'=a'\frac{\eta_P\left(\frac{M}{M_D},\frac{M_\mu}{M}\right)\eta_D\left(\frac{M_\mu}{M}\right)\varepsilon_D^{L_\mu^0}\Delta}{\langle E'_{L_\mu^0}\rangle\langle E'_{\nu_{eD}}\rangle\varepsilon_D^{\nu_{eD}}\langle\rho t\rangle},$$

and

$$a'=\left[M_\mu^7 c\tau_\mu N_A\sigma'_\nu\frac{B(D^+\to\mu^+X)}{B(D^+\to\mu^+\nu_\mu)}\right]^{-1}$$
$$=4.6\times10^{13}\ \text{cm}^{-3}\,\text{g}^{-1}\,\text{GeV}^{-6}.$$

For fixed M, it follows that

$$U_D^2\leqslant M^{-4}\sqrt{\frac{1}{C'}\frac{2.3}{f_{\nu_eD}f_{\nu_e}n_{\nu_\mu}N_{\text{POT}}}}. \tag{B20}$$

Sensitivity extends to a much lower mixing angle than that in the kaon case, essentially because the M^5 behavior of the decay rate overwhelms the $(1-M^2/M_D^2)^2$ phase-space factor in Eq. (B14), which has been incorporated with η_P. Charmed particles are also typically produced with lower energy in a hadron collision than that of kaons. This implies that L_μ^0 from charmed hadron decays will have smaller time dilation factors $E'_{L_\mu^0}/M$, and so the probability that an L_μ^0 will decay in front of the detector is larger if the L_μ^0 originates from a D^+ decay than it is for L_μ^0 from K^+ decay.

3. μ-type NHL's from D_S^+ mesons

The limit on U^2 from this source follows directly from the result for D^+ mesons since one can immediately relate the number of NHL's from D_S^+ decay to the number from D^+ decay via

$$\frac{B(D_S^+\to\mu^+L_\mu^0)}{B(D^+\to\mu^+L_\mu^0)}=\frac{V_{cs}^2M_{D_S}\left(1-\frac{M^2}{M_{D_S}^2}\right)^2f_{D_S}^2}{V_{cd}^2M_D\left(1-\frac{M^2}{M_D^2}\right)^2f_D^2}, \tag{B21}$$

and the ratio of produced $c\bar{s}$ mesons to $c\bar{d}$ mesons [18],

$$\frac{N(D_S^+)}{N(D^+)}=r_{D_SD}\simeq0.5. \tag{B22}$$

It follows that a limit on NHL's produced from D_S^+ is directly related to that from D^+ by

$$U_{D_S}^2=U_D^2\sqrt{\frac{V_{cd}^2}{V_{cs}^2}\frac{M_D\left(1-\frac{M^2}{M_D^2}\right)^2}{M_{D_S}\left(1-\frac{M^2}{M_{D_S}^2}\right)^2}\frac{f_D^2}{f_{D_S}^2}\frac{1}{r_{D_SD}}}. \tag{B23}$$

D_S^+ contribute more sensitivity to the rate than D^+ do owing do the Cabibbo-favored annihilation diagram in the former's decay. This estimate's main uncertainties are the ratio of D_S^+ to D^+ production r_{D_SD}, which is taken to be 1/2, and the ratio of pseudoscalar decay constants f_D/f_{D_S}, taken to be 1.0.

[1] OPAL Collaboration, I. DeCamp *et al.*, Phys. Lett. B **231**, 519 (1989); ALEPH Collaboration, D. DeCamp *et al.*, *ibid.* **236**, 511 (1990).

[2] See, for example, D. Wyler and L. Wolfenstein, Nucl. Phys. **B218**, 205 (1983); C.N. Leung and J.L. Rosner, Phys. Rev. D **28**, 2205 (1983).

[3] M.E. Duffy *et al.*, Phys. Rev. D **38**, 2032 (1988); WA66 Collaboration, A.M. Cooper-Sarkar *et al.*, Phys. Lett. **160B**, 207 (1985). For a summary of other experiments, see T. Wynter and L. Randall, Phys. Rev. D **50**, 3457 (1994).

[4] M. Gell-Mann, P. Ramond, and R. Slansky, in *Supergravity*, edited by D.Z. Freedman and P. van Nieuwenhuizen (North-Holland, Amsterdam, 1979), p. 315.

[5] M. Gronau, C.N. Leung, and J.L. Rosner, Phys. Rev. D **29**, 2539 (1984).

[6] J. Conrad, ''Search for Neutral Heavy Leptons in the NuTeV Experiment,'' 1995 (unpublished).

[7] CHARM Collaboration, J. Dorenbosch *et al.*, Phys. Lett. **166B**, 473 (1986).

[8] T. Bolton *et al.*, ''Precision Measurements of Neutrino Neutral Current Interactions using a Sign Selected Beam,'' Fermilab-Proposal-P-815, 1990 (unpublished).

[9] B. Lundberg *et al.*, ''Measurement of Tau Lepton Production from the Process $\nu_\tau N \rightarrow \tau$,'' Fermilab-Proposal-P872, 1994 (unpublished).

[10] DONUT estimates are from their proposal and updated numbers provided by N. Stanton (private communication).

[11] N. Armenise *et al.*, ''A New Search for $\nu_\mu \rightarrow \nu_\tau$ Oscillations,'' Report No. CERN-SPSC/90-42, 1990 (unpublished); M. de-Jong *et al.*, ''A New Search for $\nu_\mu \rightarrow \nu_\tau$ Oscillations,'' Report No. CERN-PPE/93, 1993 (unpublished).

[12] P. Astier *et al.*, ''Search for the Oscillation $\nu_\mu \rightarrow \nu_\tau$,'' Report No. CERN-SPSLC/91-21, 1991 (unpublished).

[13] K. Kodama *et al.*, ''Muon-Neutrino to Tau-Neutrino Oscillations,'' Fermilab-Proposal-P-803, 1993 (unpublished).

[14] E. Ables *et al.*, ''A Long Baseline Neutrino Oscillation Experiment at Fermilab,'' Fermilab-Proposal-P-875, 1995 (unpublished).

[15] Particle Data Group, R.M. Barnett *et al.*, Phys. Rev. D **54**, 1 (1996).

[16] B.A. Li, Phys. Rev. D **52**, 5165 (1995).

[17] P. Burchat and J. Richmond, Rev. Mod. Phys. **67**, 893 (1996).

[18] E653 Collaboration, K. Kodama *et al.*, Phys. Lett. B **286**, 187 (1992); E653 Collaboration, K. Kodama *et al.*, *ibid.* **309**, 483 (1993).